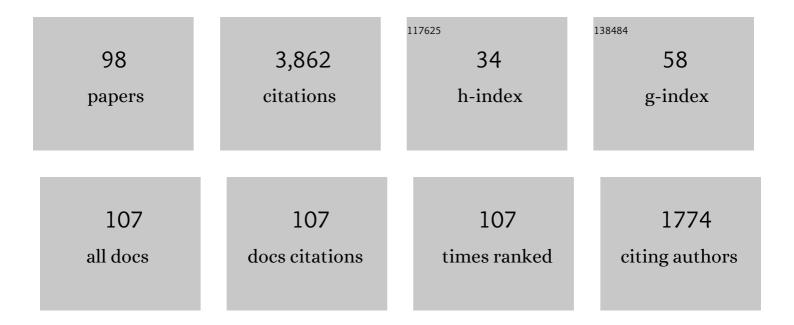
Charles C H Lin

List of Publications by Year in descending order

Source: https://exaly.com/author-pdf/1895370/publications.pdf Version: 2024-02-01



#	Article	IF	CITATIONS
1	Seismoionospheric GPS total electron content anomalies observed before the 12 May 2008 <i>M</i> _{<i>w</i>} 7.9 Wenchuan earthquake. Journal of Geophysical Research, 2009, 114, .	3.3	235
2	Theoretical study of the low- and midlatitude ionospheric electron density enhancement during the October 2003 superstorm: Relative importance of the neutral wind and the electric field. Journal of Geophysical Research, 2005, 110, .	3.3	185
3	Ionospheric disturbances triggered by the 11 March 2011 <i>M</i> 9.0 Tohoku earthquake. Journal of Geophysical Research, 2011, 116, n/a-n/a.	3.3	173
4	Motions of the equatorial ionization anomaly crests imaged by FORMOSATâ€3/COSMIC. Geophysical Research Letters, 2007, 34, .	4.0	161
5	Plausible effect of atmospheric tides on the equatorial ionosphere observed by the FORMOSAT-3/COSMIC: Three-dimensional electron density structures. Geophysical Research Letters, 2007, 34, .	4.0	158
6	Longitudinal structure of the equatorial ionosphere: Time evolution of the fourâ€peaked EIA structure. Journal of Geophysical Research, 2007, 112, .	3.3	134
7	Ionospheric GPS total electron content (TEC) disturbances triggered by the 26 December 2004 Indian Ocean tsunami. Journal of Geophysical Research, 2006, 111, .	3.3	101
8	Midlatitude summer nighttime anomaly of the ionospheric electron density observed by FORMOSATâ€3/COSMIC. Journal of Geophysical Research, 2010, 115, .	3.3	101
9	Threeâ€dimensional ionospheric electron density structure of the Weddell Sea Anomaly. Journal of Geophysical Research, 2009, 114, .	3.3	86
10	Rapid Conjugate Appearance of the Giant Ionospheric Lamb Wave Signatures in the Northern Hemisphere After Hungaâ€Tonga Volcano Eruptions. Geophysical Research Letters, 2022, 49, .	4.0	83
11	Concentric traveling ionosphere disturbances triggered by Super Typhoon Meranti (2016). Geophysical Research Letters, 2017, 44, 1219-1226.	4.0	80
12	Coseismic ionospheric disturbances triggered by the Chi hi earthquake. Journal of Geophysical Research, 2010, 115, .	3.3	78
13	Assimilation of FORMOSATâ€3/COSMIC electron density profiles into a coupled thermosphere/ionosphere model using ensemble Kalman filtering. Journal of Geophysical Research, 2012, 117, .	3.3	74
14	Observations and simulations of seismoionospheric GPS total electron content anomalies before the 12 January 2010 <i>M</i> 7 Haiti earthquake. Journal of Geophysical Research, 2011, 116, n/a-n/a.	3.3	73
15	Solar flare signatures of the ionospheric GPS total electron content. Journal of Geophysical Research, 2006, 111, .	3.3	72
16	Large-scale variations of the low-latitude ionosphere during the October-November 2003 superstorm: Observational results. Journal of Geophysical Research, 2005, 110, .	3.3	71
17	Artificial plasma cave in the low″atitude ionosphere results from the radio occultation inversion of the FORMOSATâ€3/COSMIC. Journal of Geophysical Research, 2010, 115, .	3.3	71
18	lonospheric solar flare effects monitored by the ground-based GPS receivers: Theory and observation. Journal of Geophysical Research, 2004, 109, .	3.3	67

#	Article	IF	CITATIONS
19	First tomographic observations of the Midlatitude Summer Nighttime Anomaly over Japan. Journal of Geophysical Research, 2009, 114, .	3.3	60
20	Stationary planetary wave and nonmigrating tidal signatures in ionospheric wave 3 and wave 4 variations in 2007–2011 FORMOSATâ€3/COSMIC observations. Journal of Geophysical Research: Space Physics, 2013, 118, 6651-6665.	2.4	54
21	Observational evidence of ionospheric migrating tide modification during the 2009 stratospheric sudden warming. Geophysical Research Letters, 2012, 39, .	4.0	53
22	Long-distance propagation of ionospheric disturbance generated by the 2011 off the Pacific coast of Tohoku Earthquake. Earth, Planets and Space, 2011, 63, 881-884.	2.5	52
23	Mediumâ€scale traveling ionospheric disturbances triggered by Super Typhoon Nepartak (2016). Geophysical Research Letters, 2017, 44, 7569-7577.	4.0	51
24	lonospheric assimilation of radio occultation and ground-based GPS data using non-stationary background model error covariance. Atmospheric Measurement Techniques, 2015, 8, 171-182.	3.1	49
25	Medium-scale traveling ionospheric disturbances by three-dimensional ionospheric GPS tomography. Earth, Planets and Space, 2016, 68, .	2.5	47
26	The Early Results and Validation of FORMOSATâ€7/COSMICâ€2 Space Weather Products: Global Ionospheric Specification and Neâ€Aided Abel Electron Density Profile. Journal of Geophysical Research: Space Physics, 2020, 125, e2020JA028028.	2.4	47
27	Dayside ionospheric response to recurrent geomagnetic activity during the extreme solar minimum of 2008. Geophysical Research Letters, 2010, 37, .	4.0	43
28	Ionospheric Bow Wave Induced by the Moon Shadow Ship Over the Continent of United States on 21 August 2017. Geophysical Research Letters, 2018, 45, 538-544.	4.0	43
29	Theoretical study of the ionospheric Weddell Sea Anomaly using SAMI2. Journal of Geophysical Research, 2011, 116, n/a-n/a.	3.3	42
30	The ionospheric midlatitude trough observed by FORMOSAT-3/COSMIC during solar minimum. Journal of Geophysical Research, 2011, 116, n/a-n/a.	3.3	41
31	Ionospheric data assimilation with thermosphereâ€ionosphereâ€electrodynamics general circulation model and GPSâ€TEC during geomagnetic storm conditions. Journal of Geophysical Research: Space Physics, 2016, 121, 5708-5722.	2.4	40
32	Seasonal and local time variation of ionospheric migrating tides in 2007–2011 FORMOSATâ€3/COSMIC and TIEâ€GCM total electron content. Journal of Geophysical Research: Space Physics, 2013, 118, 2545-2564.	2.4	39
33	Bow and stern waves triggered by the Moon's shadow boat. Geophysical Research Letters, 2011, 38, n/a-n/a.	4.0	37
34	Concentric traveling ionospheric disturbances triggered by the launch of a SpaceX Falcon 9 rocket. Geophysical Research Letters, 2017, 44, 7578-7586.	4.0	36
35	Tracking the epicenter and the tsunami origin with GPS ionosphere observation. Earth, Planets and Space, 2011, 63, 859-862.	2.5	35
36	Daytime longitudinal structures of electron density and temperature in the topside ionosphere observed by the Hinotori and DEMETER satellites. Journal of Geophysical Research, 2011, 116, .	3.3	34

#	Article	IF	CITATIONS
37	The summer evening anomaly and conjugate effects. Journal of Geophysical Research, 2011, 116, n/a-n/a.	3.3	33
38	Observations of global ionospheric responses to the 2009 stratospheric sudden warming event by FORMOSATâ€3/COSMIC. Journal of Geophysical Research, 2012, 117, .	3.3	33
39	Data Assimilation of Groundâ€Based GPS and Radio Occultation Total Electron Content for Global Ionospheric Specification. Journal of Geophysical Research: Space Physics, 2017, 122, 10,876.	2.4	33
40	Theoretical study of new plasma structures in the lowâ€latitude ionosphere during a major magnetic storm. Journal of Geophysical Research, 2009, 114, .	3.3	32
41	Modeling the ionospheric prereversal enhancement by using coupled thermosphereâ€ionosphere data assimilation. Geophysical Research Letters, 2017, 44, 1652-1659.	4.0	32
42	Amplitude morphology of GPS radio occultation data for sporadicâ€ <i>E</i> layers. Journal of Geophysical Research, 2012, 117, .	3.3	31
43	Thermospheric tidal effects on the ionospheric midlatitude summer nighttime anomaly using SAMI3 and TIEGCM. Journal of Geophysical Research: Space Physics, 2013, 118, 3836-3845.	2.4	30
44	Localâ€īime and Vertical Characteristics of Quasiâ€6â€Day Oscillation in the Ionosphere During the 2019 Antarctic Sudden Stratospheric Warming. Geophysical Research Letters, 2020, 47, e2020GL090345.	4.0	30
45	Ionospheric disturbances induced by a missile launched from North Korea on 12 December 2012. Journal of Geophysical Research: Space Physics, 2013, 118, 5184-5189.	2.4	29
46	Structure and origins of the Weddell Sea Anomaly from tidal and planetary wave signatures in FORMOSATâ€3/COSMIC observations and GAIA GCM simulations. Journal of Geophysical Research: Space Physics, 2015, 120, 1325-1340.	2.4	29
47	Neutral wind effect in producing a storm time ionospheric additional layer in the equatorial ionization anomaly region. Journal of Geophysical Research, 2009, 114, .	3.3	28
48	Ionospheric shock waves triggered by rockets. Annales Geophysicae, 2014, 32, 1145-1152.	1.6	28
49	Gigantic Circular Shock Acoustic Waves in the Ionosphere Triggered by the Launch of FORMOSATâ€5 Satellite. Space Weather, 2018, 16, 172-184.	3.7	28
50	A comparison of the equatorial spread F derived by the International Reference Ionosphere and the S 4 index observed by FORMOSAT-3/COSMIC during the solar minimum period of 2007–2009. Earth, Planets and Space, 2012, 64, 467-471.	2.5	26
51	Longâ€ŧerm variations of the nighttime electron density enhancement during the ionospheric midlatitude summer. Journal of Geophysical Research, 2012, 117, .	3.3	24
52	Modeling impact of FORMOSATâ€7/COSMICâ€2 mission on ionospheric space weather monitoring. Journal of Geophysical Research: Space Physics, 2013, 118, 6518-6523.	2.4	23
53	Ionosphere data assimilation modeling of 2015 St. Patrick's Day geomagnetic storm. Journal of Geophysical Research: Space Physics, 2016, 121, 11,549.	2.4	23
54	Variations in the equatorial ionization anomaly peaks in the Western Pacific region during the geomagnetic storms of April 6 and July 15, 2000. Earth, Planets and Space, 2007, 59, 401-405.	2.5	22

#	Article	IF	CITATIONS
55	A statistical study on the characteristics of ionospheric storms in the equatorial ionization anomaly region: GPSâ€TEC observed over Taiwan. Journal of Geophysical Research: Space Physics, 2013, 118, 3856-3865.	2.4	22
56	Ionospheric electron content and NmF2 from nighttime OI 135.6 nm intensity. Journal of Geophysical Research, 2011, 116, n/a-n/a.	3.3	21
57	Extreme Positive Ionosphere Storm Triggered by a Minor Magnetic Storm in Deep Solar Minimum Revealed by FORMOSATâ€7/COSMICâ€2 and GNSS Observations. Journal of Geophysical Research: Space Physics, 2021, 126, e2020JA028261.	2.4	21
58	Revisiting the Modulations of Ionospheric Solar and Lunar Migrating Tides During the 2009 Stratospheric Sudden Warming by Using Global Ionosphere Specification. Space Weather, 2019, 17, 767-777.	3.7	20
59	The Persistent Ionospheric Responses Over Japan After the Impact of the 2011 Tohoku Earthquake. Space Weather, 2020, 18, e2019SW002302.	3.7	20
60	On the Relationship Between <i>E</i> Region Scintillation and ENSO Observed by FORMOSATâ€3/COSMIC. Journal of Geophysical Research: Space Physics, 2018, 123, 4053-4065.	2.4	19
61	A statistical study of low latitude <i>F</i> region irregularities at Brazilian longitudinal sector response to geomagnetic storms during postâ€sunset hours in solar cycle 23. Journal of Geophysical Research, 2012, 117, .	3.3	18
62	Morphology of midlatitude electron density enhancement using total electron content measurements. Journal of Geophysical Research: Space Physics, 2016, 121, 1503-1517.	2.4	18
63	Ionospheric electron density inversion for Global Navigation Satellite Systems radio occultation using aided Abel inversions. Journal of Geophysical Research: Space Physics, 2017, 122, 1386-1399.	2.4	18
64	Global equatorial plasma bubble growth rates using ionosphere data assimilation. Journal of Geophysical Research: Space Physics, 2017, 122, 3777-3787.	2.4	18
65	Assimilation of Ionosphere Observations in the Whole Atmosphere Community Climate Model with Thermosphereâ€ionosphere EXtension (WACCMX). Journal of Geophysical Research: Space Physics, 2020, 125, e2020JA028251.	2.4	18
66	Seismo-Traveling Ionospheric Disturbances Triggered by the 12 May 2008 M 8.0 Wenchuan Earthquake. Terrestrial, Atmospheric and Oceanic Sciences, 2012, 23, 9.	0.6	17
67	The O I 135.6 nm airglow observations of the midlatitude summer nighttime anomaly by TIMED/GUVI. Journal of Geophysical Research, 2011, 116, n/a-n/a.	3.3	16
68	Three-dimensional electron density along the WSA and MSNA latitudes probed by FORMOSAT-3/COSMIC. Earth, Planets and Space, 2015, 67, .	2.5	16
69	Equatorial plasma bubble generation/inhibition during 2015ÂSt. Patrick's Day storm. Space Weather, 2017, 15, 1141-1150.	3.7	16
70	Observation and simulation of the ionosphere disturbance waves triggered by rocket exhausts. Journal of Geophysical Research: Space Physics, 2017, 122, 8868-8882.	2.4	16
71	lonospheric Disturbances Triggered by SpaceX Falcon Heavy. Geophysical Research Letters, 2018, 45, 6334-6342.	4.0	16
72	Conjugate Effect of the 2011 Tohoku Reflected Tsunamiâ€Driven Gravity Waves in the Ionosphere. Geophysical Research Letters, 2022, 49, e2021GL097170.	4.0	16

#	Article	IF	CITATIONS
73	Spaceâ€based imaging of nighttime mediumâ€scale traveling ionospheric disturbances using FORMOSATâ€2/ISUAL 630.0 nm airglow observations. Journal of Geophysical Research: Space Physics, 2016, 121, 4769-4781.	2.4	15
74	Lunar Tide Effects on Ionospheric Solar Eclipse Signatures: The August 21, 2017 Event as an Example. Journal of Geophysical Research: Space Physics, 2020, 125, e2020JA028472.	2.4	15
75	The Equatorial El Niño-Southern Oscillation Signatures Observed by FORMOSAT-3/COSMIC from July 2006 to January 2012. Terrestrial, Atmospheric and Oceanic Sciences, 2014, 25, 545.	0.6	14
76	Observation and Simulation of the Development of Equatorial Plasma Bubbles: Post‣unset Rise or Upwelling Growth?. Journal of Geophysical Research: Space Physics, 2020, 125, e2020JA028544.	2.4	13
77	Advances in Ionospheric Space Weather by Using FORMOSAT-7/COSMIC-2 GNSS Radio Occultations. Atmosphere, 2022, 13, 858.	2.3	12
78	Global Ionospheric Structure Imaged by FORMOSAT-3/COSMIC: Early Results. Terrestrial, Atmospheric and Oceanic Sciences, 2009, 20, 171.	0.6	11
79	First results of the limb imaging of 630.0 nm airglow using FORMOSATâ€2/Imager of Sprites and Upper Atmospheric Lightnings. Journal of Geophysical Research, 2009, 114, .	3.3	10
80	Using the IRI, the MAGIC model, and the co-located ground-based GPS receivers to study ionospheric solar eclipse and storm signatures on July 22, 2009. Earth, Planets and Space, 2012, 64, 513-520.	2.5	10
81	Critical Issues in Ionospheric Data Quality and Implications for Scientific Studies. Radio Science, 2019, 54, 440-454.	1.6	10
82	FORMOSAT-3/COSMIC observations of the ionospheric auroral oval development. GPS Solutions, 2010, 14, 91-97.	4.3	9
83	Statistical study of medium-scale traveling ionospheric disturbances in low-latitude ionosphere using an automatic algorithm. Earth, Planets and Space, 2021, 73, .	2.5	9
84	Ionospheric plasma caves under the equatorial ionization anomaly. Journal of Geophysical Research, 2012, 117, .	3.3	8
85	Numerical Modeling of the Concentric Gravity Wave Seeding of Lowâ€Latitude Nighttime Mediumâ€Scale Traveling Ionospheric Disturbances. Geophysical Research Letters, 2018, 45, 6390-6399.	4.0	8
86	Ionospheric Electron Density Concurrently Derived by TIP and GOX of FORMOSAT-3/COSMIC. Terrestrial, Atmospheric and Oceanic Sciences, 2009, 20, 207.	0.6	7
87	Plasma Depletion Bays in the Equatorial Ionosphere Observed by FORMOSATâ€3/COSMIC During 2007–2014. Journal of Geophysical Research: Space Physics, 2020, 125, e2019JA027501.	2.4	6
88	Near Realâ€Time Global Plasma Irregularity Monitoring by FORMOSATâ€7/COSMICâ€2. Journal of Geophysical Research: Space Physics, 2021, 126, .	2.4	6
89	Theoretical study of the ionospheric plasma cave in the equatorial ionization anomaly region. Journal of Geophysical Research: Space Physics, 2014, 119, 10,324.	2.4	5
90	Lowâ€latitude midnight brightness in 630.0 nm limb observations by FORMOSATâ€2/ISUAL. Journal of Geophysical Research: Space Physics, 2014, 119, 4894-4904.	2.4	5

#	Article	IF	CITATIONS
91	The fast development of solar terrestrial sciences in Taiwan. Geoscience Letters, 2016, 3, .	3.3	5
92	Modeling study of the ionospheric responses to the quasi-biennial oscillations of the sun and stratosphere. Journal of Atmospheric and Solar-Terrestrial Physics, 2018, 171, 119-130.	1.6	5
93	Implication of Tidal Forcing Effects on the Zonal Variation of Solstice Equatorial Plasma Bubbles. Journal of Geophysical Research: Space Physics, 2021, 126, e2020JA028295.	2.4	5
94	Equatorial ionization anomaly response to lunar phase and stratospheric sudden warming. Scientific Reports, 2021, 11, 14695.	3.3	4
95	Coordinated Observations of Rocket Exhaust Depletion: GOLD, Madrigal TEC, and Multiple Lowâ€Earthâ€Orbit Satellites. Journal of Geophysical Research: Space Physics, 2022, 127, .	2.4	4
96	Comparison of FORMOSATâ€3/COSMIC radio occultation measurements with radio tomography. Radio Science, 2011, 46, .	1.6	3
97	The impact of FORMOSAT-5/AIP observations on the ionospheric space weather. Terrestrial, Atmospheric and Oceanic Sciences, 2017, 28, 129-137.	0.6	3
98	A Statistical Comparison of Zonal Mean and Tidal Signatures in FORMOSAT-3/COSMIC and Ground-Based GPS TECs. Terrestrial, Atmospheric and Oceanic Sciences, 2013, 24, 253.	0.6	1